4

Low-Temperature Experiments and Proposals

4.1 Introduction

Several independent groups are currently investigating low-temperature ($T \leq 10K$) second law challenges that exploit uniquely quantum mechanical behaviors. Two of these invoke the phase transition from normal to superconducting states and are currently under active experimental investigation (§4.3, §4.4), while others rely on quantum entanglement and constitute theoretical proposals for experiments (§4.6). We begin with a brief review of superconductivity.

4.2 Superconductivity

4.2.1 Introduction

Superconductivity is a macroscopic quantum phenomenon. The first and most obvious evidence of it is the Meissner effect discovered by Meissner and Ochsenfeld in 1933 when they observed that a superconductor in a weak magnetic field completely expels the field from the superconducting bulk except for a thin layer at the surface [1]. This is a more fundamental aspect of superconductivity than the disappearance of electrical resistance[1], first discovered in mercury at low temperatures by Kamerlingh Onnes in 1911. Superconductivity is a state with long-range

[1] Electrical resistance is effectively zero ($\rho < 10^{-26}\Omega$m).

phase correlations, which are a consequence of Bose-Einstein condensation of electron pairs [2, 3, 4]. Pairs of electrons (fermions individually) form Cooper pairs (which are bosons) via electron-phonon-electron interactions, as described by the Bardeen-Cooper-Schrieffer theory [5].

Complete flux expulsion in the simple form of the Meissner effect occurs only in weak magnetic fields. If the applied field is sufficiently strong and if demagnetization becomes appreciable, then magnetic flux penetrates through the superconductor. This penetration differentiates the two types of superconductors, which have differing signs of the wall energy associated with the interface between the normal and superconducting domains. In Type-I superconductors the wall energy is positive and, therefore, the magnetic flux contained in a single normal domain consists of many flux quanta. (One magnetic flux quantum ($\Phi_o = \frac{h}{2q}$) is the smallest unit of magnetic flux.) Type-II superconductors are characterized by negative interface boundary surface energy (wall energy). In this case, magnetic flux can be distributed through the superconductor such as to form either normal regions or a mixed phase of superconducting and normal regions. The particular type of superconductivity is determined by a parameter κ of the Ginzburg-Landau theory [6]: at $\kappa < 1/\sqrt{2}$ the wall energy of a normal-superconducting interface is positive and the superconductor is Type-I, while at $\kappa > 1/\sqrt{2}$ the wall energy is negative and the superconductor is Type-II. The Ginzburg-Landau parameter $\kappa = \lambda(T)/\xi(T)$ relates the two characteristic lengths of superconductor: the penetration depth $\lambda(T)$ and the coherence length $\xi(T)$. These have similar temperature dependences

$$\xi(T) \approx \xi_0[1 - (\frac{T}{T_c})^4]^{-1/2}$$

$$\lambda(T) \approx \lambda_0[1 - (\frac{T}{T_c})^4]^{-1/2} \tag{4.1}$$

The penetration depth λ_0, the scale length over which an external magnetic field can penetrate into the superconductor, depends only on the density of superconducting pairs. The coherence length, ξ_0, is the maximum scale length over which Cooper pairs interact, or equivalently, it is the scale length over which superconductivity can be established or destroyed. ξ_0 decreases with the electron mean free path in dirty superconductors. Type-II superconductivity occurs preferentially in alloys or, more generally, in impure systems. Pure metals usually display Type-I superconductivity. The penetration depth has approximately the same value $\lambda_0 \approx 10^{-8} - 10^{-7}$m for most superconductors, whereas the coherence length may run from $\xi(0) \approx 10^{-6}$m in pure aluminium [7] down to $\xi(0) < 10^{-9}$m in high temperature superconductors [8].

The free energy of the superconducting phase $f_s(T)$ is less than that of the normal phase $f_n(T)$ for temperatures lower than the critical one $T < T_c$. The superconductor's exclusion of magnetic flux increases its free energy density by $\frac{\mu_0 H^2}{2}$: the price of diagmagnetism. The magnetic field H_c at which the free energy gain associated with electron condensation into Cooper pairs equals the free energy cost of its diamagnetism, $f_n(T) - f_s(T) = \frac{\mu_0 H_c^2}{2}$ [9], is called the thermodynamic critical field. There is another critical field, $H_{c2} = \sqrt{2}\ \kappa H_c$, called second critical

field [9]. According to the Abrikosov theory [10] the transition between the normal and superconducting vortex state of Type-II superconductors takes place at this critical field $H_{c2} = \sqrt{2}\ \kappa H_c > H_c$. However, in reality, this transition is observed below H_{c2} [11, 12, 13]. Samples of Type-I superconductors (for which $\sqrt{2}\ \kappa < 1$) undergo transition between normal and superconducting phases at $H_c > H_{c2} = \sqrt{2}\ \kappa H_c$ when their size or demagnetization coefficient are enough small. In the opposite case of a finite demagnetization coefficient D, the intermediate state is observed at $H_c(1 - D) < H < H_c$. This state is a configuration consisting of a mixture of normal and superconducting domains [9]. The critical field H_c, above which superconductivity of Type-I superconductors disappears, has been found to follow, to good approximation, the empirical relation

$$H(T) = H_c[1 - (\frac{T}{T_c})^2]. \tag{4.2}$$

Type-I superconductors have critical fields $H_c \leq 0.2$T, whereas low-temperature Type-II superconductors with high values of the Ginzburg-Landau parameter κ have $H_{c2} = \sqrt{2}\ \kappa H_c$ up to 50 T. High-temperature ceramic superconductors have the second critical fields up to several hundred Teslas.

4.2.2 Magnetocaloric Effect

In non-zero fields, the normal-superconducting transition of Type-I superconductor is first order and has an associated latent heat. A sample heats (cools) when making the transition *to* the superconducting (normal) state. This is the magnetocaloric effect. (A non-quantum mechanical electrostatic analog, the electrocaloric effect, is employed by Trupp in another second law challenge (§5.5 and [14]).

Although superconductors are perfect diamagnets, excluding magnetic flux from their bulk interiors, surface-parallel fields penetrate shallowly into their outer layers, decaying exponentially in strength with a characteristic *penetration depth* (see (4.1)); that is, $H(z) = H_o e^{-z/\lambda}$. Note that $\lambda \to \infty$ as $T \to T_c$ since $\lambda \propto 1/\sqrt{n_s}$ [9], where $n_s \propto T_c - T$ is the density of superconducting pairs; that is, as the penetration depth becomes large at the transition temperature, the sample becomes normal.

During transition between normal to superconducting phases, a sample usually passes through an *intermediate state* wherein lamellae of normal phase riddle the superconducting bulk. Samples of suitably small size ($\xi \geq d \geq 5\lambda$) can undergo the normal-to-superconducting transition en masse, without passing through an intermediate state. Given the inherently small sizes of ξ and λ, d is narrowly restricted to roughly $10^{-6}\text{m} \geq d \geq 10^{-7}\text{m}$. In such a transition, there can be no lamellae and the sample instantaneously can snap from one thermodynamic equilibrium to the other. Type-I elemental superconductors that fit this criterion include Sn ($(\xi/\lambda) = 4.5$), In ($(\xi/\lambda = 6.9$), and Al ($(\xi/\lambda) = 32$).

Whereas the intermediate state observed in large samples of Type-I superconductors have been investigated in detail [9], the thermodynamics of small samples has not been well studied thus far. Although Pippard raised questions about

the irreversible effects in the magnetization cycle of superconducting colloids as early as 1952 [15], up to now there has been little experimental work devoted to the magnetization and transition between normal and superconducting states of small samples of Type-I superconductors. The resistive measurements of thin tin whiskers made by Lutes and Maxwell as early as 1955 [16] show that an abrupt transition from the superconducting to normal state can occur without the intermediate state in samples of suitably small size. But only recently have techniques been developed [17] that allow quantitative studies of thermodynamic properties of individual superconducting particles at micron and sub-micron scale lengths. The results of [18] demonstrate the irreversible effects in the magnetization cycle of Al disks down to diameter $> 0.3\ \mu m$ [17]. However, it is important to emphasize that this irreversibility is conditioned by a high value of demagnetization coefficient typical of thin disks. Reversible behaviour can be expected only in small samples with geometries like spheres.

The combination of the magnetocaloric effect with reversible transition renders the *coherent magnetocaloric effect* (CMCE). This is the key new insight underlying Keefe's second law challenge. Inherently, this is a quantum mechanical process that relies on the superconductor's long-range order parameter (wavefunction).

4.2.3 Little-Parks (LP) Effect

The Meissner effect is a quantum phenomena arising from the quantization of momentum circulation of superconducting pairs. The generalized momentum of a charge q is given by $p = mv + qA$, where A is the magnetic vector potential. For Cooper pairs $q \longrightarrow 2e$, where e is the charge of the electron. The quantization of momentum circulation along a closed path is [2]

$$\oint p\ dl = nh = \oint mv\ dl + \oint 2eA\ dl = m \oint v\ dl + 2e\Phi, \tag{4.3}$$

where n is equal to zero for any closed path inside a simply-connected superconductor without a singularity in its wavefunction. Therefore, the persistent electrical current $j_p = 2evn_s$ should be maintained in outer layers of a superconductor (where the velocity of superconducting pairs v is determined by the relation $m \oint v\ dl + 2e\Phi = 0$), while in its interior bulk, where $v = 0$, the magnetic flux should be absent ($\Phi = 0$).

For a closed path in a multiply-connected superconductor — for example in a loop — the integer n in (4.3) can be any value and the velocity circulation of Cooper pairs should be

$$\oint v\ dl = \frac{h}{m}\left[n - \frac{\Phi}{\Phi_o}\right] \tag{4.4}$$

where $\Phi_0 = h/2e$ is the flux quantum (fluxoid). The magnetic flux inside the loop is $\Phi = BS + LI_p$, where B is the magnetic induction induced by an external magnet; S is the area of the loop; L is the inductance of the loop; $I_p = sj_p = s2evn_s$ is the persistent current around the loop. The velocity (4.4) and the persistent

current of the loop with weak screening ($LI_p < \Phi_0$) is a periodic function of the magnetic flux $\Phi \approx BS$ since velocity circulation (4.4) cannot be zero unless $\Phi = n\Phi_0$ and the thermodynamic average value of the quantum number n is close to an integer number n corresponding to minimum kinetic energy Cooper pairs, *i.e.*, to minimum $\mathcal{E} \propto v^2 \propto (n - \Phi/\Phi_0)^2$. This quantum periodicity leads to experimentally observable effects.

The first such effect was observed by Little and Parks in 1962 [19]. The quantum periodicity in the transition temperature T_c of a superconducting cylinder [19] or a loop [20] from enclosed magnetic flux following Φ was explained as a consequence of the periodic dependence of the free energy [19, 21, 2]: $\Delta T_c \propto -\mathcal{E} \propto -v^2 \propto -(n - \Phi/\Phi_0)^2$. For a cylinder or loop with a radius R, the dependence of critical temperature with flux varies as

$$T_c(\Phi) = T_c \left[1 - (\frac{\xi(0)}{R})^2 (n - \frac{\Phi}{\Phi_o})^2\right], \tag{4.5}$$

where $\xi(0)$ is its coherence length at $T = 0$. The values of $(n - \Phi/\Phi_0)$ is constrained between -0.5 and 0.5. The relation (4.5) describes well the experimental dependencies $T_c(\Phi)$ obtained from resistive measurements [19, 2, 20].

This explanation of the Little-Parks (LP) effect is not complete, however. It does not explain, for instance, why the persistent current I_p has been observed at non-zero resistances ($R > 0$) in a number of studies. It is emphasized that the observation of a persistent current I_p — *i.e.*, a direct current observed under thermodynamic equilibrium conditions, at a non-zero resistance $R > 0$ — contradicts standard expectations since it implies power dissipation (RI_p^2) and, by inference, a direct current power source under equilibrium conditions. Nikulov advances this as evidence for the potential violability of the second law.

Nikulov's key insight is to reinterpret and extend the results of the LP experiments to consideration of inhomogeneous superconducting loops immersed in magnetic fields near their transition temperatures. From these he concludes that thermal fluctuations can be used to drive electrical currents in the presence of nonzero resistance, and by this achieve nonzero electrical dissipation at the expense of thermal fluctuations alone. In essence, thermal energy is rectified into macroscopic currents, this in violation of the second law. Nikulov proposes a new force, the *quantum force* — which arises from the exigencies of the quantum-to-classical, superconducting-to-normal transition — to explain these fluctuation-induced currents [22]

4.3 Keefe CMCE Engine

4.3.1 Theory

Keefe proposes a simple thermodynamic process in which a small superconducting sample is cycled through field-temperature (H-T) space and performs net work solely at the expense of heat from a heat bath [23, 24]. (We use Keefe's nomen-

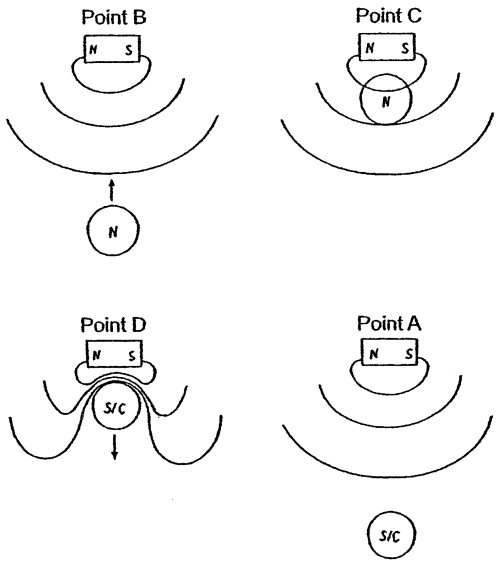

Figure 4.1: Pictorial overview of CMCE cycle.

clature.) It incorporates facets of other standard H-T cycles [25, 26], but also uniquely invokes the coherent magnetocaloric effect (CMCE).

The cycle is given pictorially and graphically in Figures 4.1 and 4.2. Figure 4.1 pictures a small armature of superconductor (meeting CMCE requirements) moving in and out of a magnetic field during a full thermodynamic cycle. Here "N" and "S/C" indicate normal and superconducting states. Figure 4.2 graphs the armature's progress in H-T space and indicates work and heat influxes and effluxes.

The cycle begins with the armature (volume V) in the superconducting state (point A in Figure 4.2) at thermodynamic coordinates (T_1, H_1). Until otherwise noted, the armature is thermally insulated and the process proceeds adiabatically.

The armature is moved slightly closer to the magnet, thus increasing the magnetic field it experiences, so it passes to the normal side of the critical field (Tuyn) curve (point B, Figure 4.2) with coordinates (T_1, $H_1 + \Delta H$). (The magnetodynamic work to move the armature is assumed to be zero.) The armature coherently transitions to the normal state, evolves latent heat (LH_1) and magnetocalorically cools to T_2, given through

$$LH_1 = T_1(S_{n1} - S_{s1}) = V \cdot \int_{T_1}^{T_2} C_n dT \tag{4.6}$$

With precisely orchestrated motion, the armature moves inwardly toward the magnet as it cools (Process B, Figure 4.1) so as to skirt the normal side of the Tuyn curve ($B \rightarrow C$, Fig 2.). The armature, now fully cooled (point C, Figure 4.2) at coordinates (T_2, H_2), is removed slightly out of the field, thus reducing its

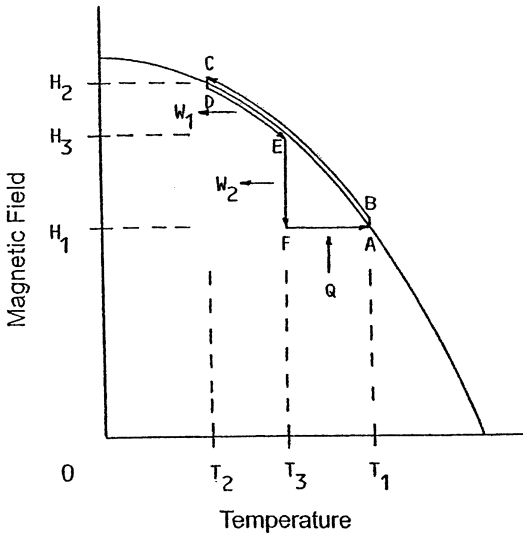

Figure 4.2: Coherent magnetocaloric effect (CMCE) cycle on H-T phase diagram.

field to $H_2 - \Delta H$, and thereby crossing it back to the superconducting side of the Tuyn curve (point D, Figure 4.1) at coordinates (T_2, $H_2 - \Delta H$). Latent heat is evolved, magnetocalorically heating the armature to T_3, given via

$$LH_2 = T_2(S_{n2} - S_{s2}) = V \cdot \int_{T_2}^{T_3} C_s dT \tag{4.7}$$

Now on the superconducting side of the Tuyn curve again, the Meissner effect kicks in and forcibly expels the magnetic field from the interior of the armature, whereupon the armature is repelled out of the high field region near the magnet. During its forcible expulsion (path $D \rightarrow E$, Figure 4.2), the armature performs work

$$W_1 = \frac{\mu_o(H_2^2 - H_3^2)}{2} \cdot V \tag{4.8}$$

Similarly as for path segment $B \rightarrow C$ in Figure 4.2, the armature moves in a precisely timed and coordinated fashion from $D \rightarrow E$ so as to skirt the superconducting side of the Tuyn curve while magnetocalorically heating to T_3 (and also while simultaneously performing work). From point E (Figure 4.2), the superconducting armature is moved further out of the field (Process D, Figure 4.1), performing additional work

$$W_2 = \frac{\mu_o(H_3^2 - H_1^2)}{2} \cdot V \tag{4.9}$$

and arrives at point F (Figure 4.2) with coordinates (T_3, H_1).

Up to this point, processes have been adiabatic. From $F \rightarrow A$ (Fig 2), however, the superconducting armature is thermally coupled to the surrounding heat bath (T_1) and heats ($T_3 \rightarrow T_1$), thus closing the cycle and absorbing heat

$$Q = V \cdot \int_{T_3}^{T_1} C_s dT. \tag{4.10}$$

As described, heat transfer occurs only in the final step of the cycle; here heat is absorbed. Since positive work is performed by the armature elsewhere in the cycle, if the cycle operates in steady-state, the first law implies that the heat absorbed from the heat bath is transformed into work.

Keefe calculated the net work per cycle expected for an exemplary tin armature and cycle [27]. The cycle is specified by the vertex coordinates in Figure 4.2. In terms of tin's critical field (H_c) and the critical temperature (T_c), these are: (T_1, H_1) = ($0.6T_c$, $0.64H_c$), (T_2, H_2) = ($0.186T_c$, $0.965H_c$), (T_3, H_3) = ($0.407T_c$, $0.834H_c$). For this cycle, the latent heat densities are: $LH_1 = 340$ J/m^3, $LH_2 = 50$J/m^3. The work density/cycle is: $W_1 = 88$J/m^3, $W_2 = 107$J/m^3, and the heat density/cycle is: $Q = 195$J/m^3. Satisfying the first law, $W_1 + W_2 = Q$, implies for the second:

$$\Delta S = -\int_{T_3}^{T_1} \frac{dQ(T)}{T} dT < 0 \tag{4.11}$$

In principle, net work can be extracted from the CMCE cycle mechanically (*e.g.*, motor), electronically (*e.g.*, generator), or via a heat pump. Given the theoretical limitation to small armatures, usable power would probably be extracted in large arrays. Since operating frequencies for mechanical devices of this size can be high ($f \sim 10^9 - 10^{12}$Hz), high output power densities might be achieved [28]. For example, assuming an individual tin CMCE motor is 10 times larger (10^3 times greater volume) than its armature ($d \simeq 10^{-7}$m) and operates at $f = 10^{10}$Hz, based on tin's calculated work density/cycle, its power density is estimated to be $\mathcal{P} \simeq f(W_1 + W_2) \simeq 2 \times 10^{12}$W/m^3.

4.3.2 Discussion

The movement of normal phase electrons through the external magnetic field should generate eddy currents, Ohmic heating, and entropy, with magnitude dependent on the rapidity of movement. The armature's coherent transition time could be quite short, perhaps shorter than 10^{-12}s (*i.e.*, 10^{-4} the light travel time across the armature) and the resultant latent heat should manifest itself as a temperature change within a few vibrational periods of the lattice ($\tau_{lattice} \sim 10^{-13}$s), therefore, the armature must cycle quickly to faithfully trace the Tuyn curve, perhaps at THz frequencies. At these frequencies, one expects eddy current heating of the normal electrons (and perhaps even of the superelectrons). Normal electrons are known to interact with ac fields, causing dissipation and entropy production in superconducting samples. Superelectrons can absorb electromagnetic radiation

near the necessary projected operating frequency of the armature. Magnetic dipole radiation could also be significant.

The physical magnet giving rise to the armature's external magnetic field should experience a back reaction and possibly internal induced electric fields and dissipation due to the rapid and possibly sizable distortions of field by the action of the armature. Given its small size, account should be taken of thermal fluctuations and whether these might drive it inopportunely across the transition line. Hysteresis should also be considered [29]. Finally, the sophistication in microscopic mechanical engineering required to realize a working CMCE engine is beyond the present state of the art in micro- or nanomanufacturing, but may be on the horizon.

Experiments are currently being pursued in Moscow, Russia to understand better the CMCE effect as it pertains to Keefe's engine. While falling short of an actual engine test, they are laying necessary foundations. Indium spheres ($r \simeq 1.25 \times 10^{-7}$m, $T_c = 3.7$K, $\xi/\lambda = 6.9$) will be analysed with a ballistic Hall micromagnetometer as the sample is cycled through the normal-superconducting transition ($2.5\text{K} \leq T \leq 3\text{K}$). Keefe, et al. will check predicted values of the transition field, the transition time scale, and investigate hysteresis, which can diminish the efficiency of the thermodynamic cycle. Tight control of the sphere size and purity will be necessary since the CMCE effect is predicted to be robust only within a narrow range of particle sizes.

In summary, the CMCE cycle appears theoretically compelling despite many uncertainties surrounding superconducting and quantum processes in the mesoscopic regime. Experimental considerations are problematic, but are currently being investigated. The technical challenges in fabricating a working mechanical CMCE engine are formidable.

4.4 Nikulov Inhomogeneous Loop

Over the last seven years, Zhilyaev, Dubonov, Nikulov, et al. have conducted laboratory experiments that corroborate the essential features of Nikulov's theory. Recent independent theoretical analysis by Berger [30] also lends support to his position. We introduce this challenge through Nikulov's quantum force.

4.4.1 Quantum Force

Nikulov's proposed quantum force arises from the fundamental differences between classical and quantum states of electrons (or Cooper pairs) in a conducting (superconducting) loop. In their classical state, electrons occupy a continuous energy spectrum. Direct current cannot exist at equilibrium according to classical mechanics because the equilibrium distribution function f_0 for electrons depends on v quadratically through kinetic energy $f_0(v^2)$ such that the average thermodynamic current $j_{av} = q\sum_p v f_0$ for this continuous distribution is an odd integral

$j_{av} = q \int v f_0 dv$, which is equal to zero.

In contrast, in quantum mechanics a persistent current j_{pc} can exist — *i.e.*, direct current observed under equilibrium conditions — since the discrete sum

$$j_{pc} = q \sum_p v f_o(\frac{E(p)}{kT}) = \frac{q}{m} \sum_p (p - qA) f(\frac{E(p)}{kT}) \tag{4.12}$$

cannot be replaced by a continuous integral as in the classical case. The energy difference between permitted states for a superconducting loop

$$E_p = s \oint 2n_s(\frac{mv_s^2}{2})dl = \frac{sh}{4lm\langle n_s^{-1}\rangle} \left[n - \frac{\Phi}{\Phi_o}\right]^2 \tag{4.13}$$

is much higher than the thermal energy $\Delta\mathcal{E} = \mathcal{E}(n+1) - \mathcal{E}(n) \approx sh/4lm\langle n_s^{-1}\rangle \gg kT$ in the closed superconducting state, when $\langle n_s^{-1}\rangle^{-1} = (l^{-1} \oint_l dl n_s^{-1})^{-1} \approx n_s$, since the number of Cooper pairs sln_s is very large for any realistic superconducting loop [22]. (Here s and l are the cross-sectional area and length of the loop wire and n_s is the number density of Cooper pairs.)[2] Thus, a transition between the discrete spectrum, with well-spaced energy states $\Delta\mathcal{E} = \mathcal{E}(n+1) - \mathcal{E}(n) \gg kT$, and the continuous spectrum $\Delta\mathcal{E} = 0$ takes place when a loop is switched between superconducting states with different connectivity. The velocity v_s and the momentum p of Cooper pair change at this transition: $\oint_l p_{cl} dl = nh$ and the velocity is defined by (4.4) in the closed superconducting state, whereas in the open superconducting state $v_s = 0$ and $\oint_l p_{un} dl = 2e\Phi$. The momentum circulation changes from $2e\Phi$ to nh at closing of the superconducting state because of the flux quantization: $nh - 2e\Phi = h(n - \Phi/\Phi_0)$. The time rate of change of the momentum due to reiterated switching of the loop between superconducting states (at frequency f) is a force given by

$$\oint F_q dl = \oint (p_{cl} - p_{un}) f dl = h(\langle n\rangle - \frac{\Phi}{\Phi_0}) f. \tag{4.14}$$

This is coined the *quantum force* [22], $F_q = (p_{cl} - p_{un})f$. Here $\langle n\rangle$ is the thermodynamic average of the quantum number n.

The reiterated switching can be induced by external current [31], by external electrical noise [32], or by equilibrium thermal fluctuations [22]. The quantum force induced by thermal fluctuations is the Langevin force [33, 34]. It maintains the persistent current in the presence of a damping force (dissipation via electrical resistance) just as the classical Langevin force maintains the Nyquist's noise current in a classical normal metal loop. In contrast with the classical Langevin force, however, the average value of the quantum force is not equal to zero at $\Phi = n\Phi_0$ and $\Phi = (n + 0.5)\Phi_0$, when $\langle n\rangle - \Phi/\Phi_0 \neq 0$. Therefore, the persistent current at $R > 0$ is an ordered Brownian motion with non-zero direct component, this in contradistinction to Nyquist's noise, which is completely chaotic. According to

[2] The energy difference $\Delta\mathcal{E} = \mathcal{E}(n+1) - \mathcal{E}(n) \approx sh/4lm\langle n_s^{-1}\rangle = 0$ in the open superconducting state since $\langle n_s^{-1}\rangle^{-1} = 0$ when the density of Cooper pairs equals zero $n_s = 0$ in any loop segment. As expected, no current flows in this case.

Nikulov, this phenomenon violates the postulate of randomness under equilibrium conditions, the same that saved the second law of thermodynamics at the beginning of 20^{th} century. Nikulov claims that $I_p \neq 0$ at $R > 0$ is evidence of persistent power generation RI_p^2, the existence of which conflicts with the second law [33, 34]. The first experimental evidence of this phenomenon is, apparently, the original LP experiment itself over 40 years ago [19, 20] — and, therefore, arguably it represents the first experimentally-based second law challenge.

4.4.2 Inhomogeneous Superconducting Loop

By analogy with well-known theoretical and experimental results for normally conductive loops with inhomogeneous (asymmetric) resistivity, voltage oscillations are expected on a segment l_s of an inhomogeneous superconducting loop, satisfying

$$V(\frac{\Phi}{\Phi_0}) = \left[\frac{R_{ls}}{l_s} - \frac{R_l}{l}\right] l_s I_p(\frac{\Phi}{\Phi_0}) \tag{4.15}$$

Here R_{ls} and l_s are the resistance and length of a loop segment; R_l and l are the resistance and length of the whole of the loop, and I_p is the persistent current. Experimental results corroborate this [31, 32]. The quantum analogy to the classical electrical case appears valid since the quantum force is uniform around the loop [22] just as the Faraday 'voltage' $-d\Phi/dt$ is uniform around a conventional loop.

Segments of a superconducting loop can have different resistances $R_{ls}/l_s \neq R_l/l \neq 0$ at nonzero currents $I_p \neq 0$ if they are in the normal state at different times when the loop is switched between superconducting states with different connectivity. This is possible if loop segments, for example l_a and l_b, have distinct critical temperatures, specifically $T_{ca} > T_{cb}$ (See Figure 4.3.). The limiting case is when one segment (l_b) is switched between superconducting and normal states while the other segment l_a (with $l_a + l_b = l$) remains always in the superconducting state (therefore, with $R_a = 0$ and $R = R_b$). This was considered by Nikulov in [35]. A flat ($h < R$) and narrow ($w \ll R$) loop with $h, w < \lambda$ was analysed. He found that the direct potential difference V_b [35]

$$V_b = R_b I_p \simeq (\frac{l_b\langle n_{sb}\rangle}{l_b n_{sa} + l_a\langle n_{sb}\rangle}) \cdot (\frac{n\Phi_o - \Phi}{\lambda_{La}^2})\rho_b \tag{4.16}$$

can be observed if the average value of the Cooper pair density $\langle n_{sb}\rangle$ and resistivity ρ_b of the l_b segment do not equal zero; *i.e.*, if the segment is switched between superconducting and normal states. Here $\lambda_{La} = (m/4e^2 n_{sa})^{1/2}$ is the London penetration length for segment l_a. Relation (4.16) is valid for high switching frequency ($f \gg R_b/L$). At a low frequency ($f \ll R_b/L$), the amplitude of the quantum oscillations of the dc voltage with respect to the magnetic field $V_b(\Phi/\Phi_0)$ is proportional to the switching frequency f [35, 22] and is given by

$$V_b = \frac{hf}{2e}(\langle n\rangle - \frac{\Phi}{\Phi_0})\frac{l_b}{l}. \tag{4.17}$$

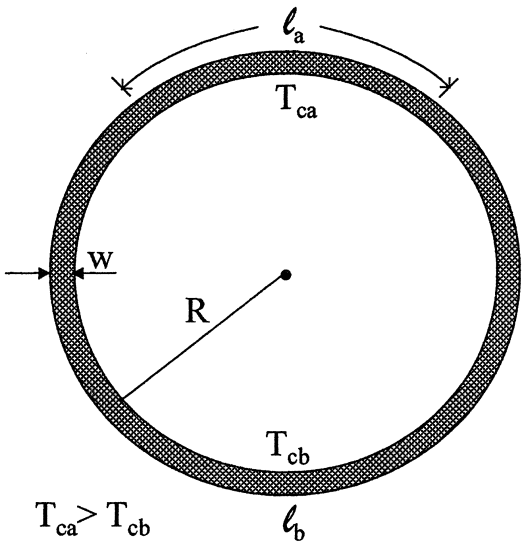

Figure 4.3: Schematic of inhomogeneous mesoscopic superconducting loop with different critical temperatures on segments a and b.

The correlation between the dc voltage and the frequency is similar to that of Josephson [36, 32].

The crux of this second law challenge [35, 22] lies in the switching of the l_b segment by thermal fluctuations at $T \approx T_{cb}$. In this case, V_b is the persistent voltage $V_b \equiv V_p$ and $\mathcal{P}_p = I_p V_p = R_b I_p^2 = V_p^2/R_b$ is the persistent power [37]. It can be shown in that the persistent power $\mathcal{P}_p$ of a single loop cannot exceed the total power of thermal fluctuations [35, 37, 22]:

$$\mathcal{P}_{thermal} \simeq \frac{(kT)^2}{\hbar}. \tag{4.18}$$

According to (4.18), the persistent power of a single mesoscopic loop made from a high-temperature superconductor (HTSC) with $T_c \simeq 100$K is expected to be quite small; *i.e.*, $\mathcal{P}_p < \mathcal{P}_{thermal} \simeq 10^{-8}$W, while for a low-temperature superconductor ($T_c \simeq 10$)K, one expects even less power: $\mathcal{P}_p < \mathcal{P}_{thermal} \simeq 10^{-10}$W. (Notice that in (4.18), power scales as T^2.) However, since power sources can be stacked, multiple inhomogeneous loops can be arranged in series such that their voltage V_p and power $\mathcal{P}_p$ add. A series of $N = 10^8$ HTSC loops could, in theory, achieve dc power up to $\mathcal{P}_p < N(kT)^2/\hbar \simeq 1\ W$ [34] in an area $\approx 1\text{cm}^2$. Power densities of the order of 10^8W/m^3 might be possible [34].

In principle, the persistent voltage V_b can be measured experimentally even on a single loop of low-temperature superconductor; one expects $V_b < R_b((kT)^2/\hbar)^{0.5} \approx 10\mu V$ at $T \simeq 1\ K$ and $R_b \simeq 10\ \Omega$. For high-temperature superconductors and loops in series, V_b could be an order of magnitude greater. These voltages are the primary objects of experimental study.

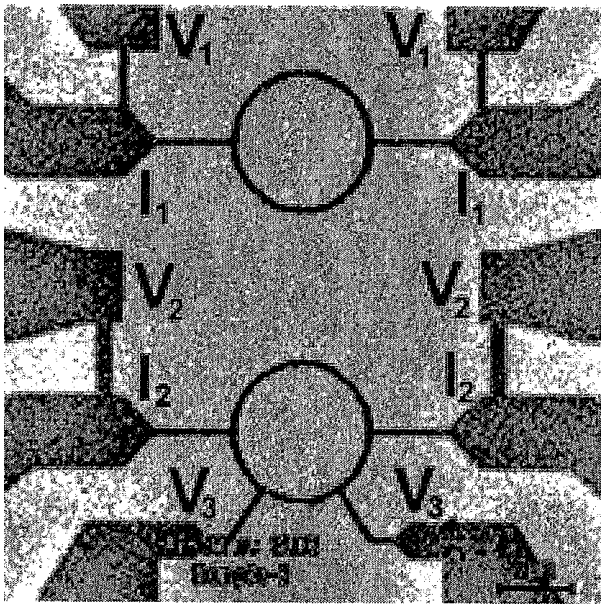

Figure 4.4: Electron micrograph of Series I experiments' symmetric (top) and asymmetric (bottom) mesoscopic aluminum loops. I_j and V_j are current and voltage contacts for each loop. Additional V_3 contacts on lower loop.

4.4.3 Experiments

Experiments investigating Nikulov's paradoxical effect date to 1997 with unpublished observations by I.N. Zhilyaev of dc voltages on segments of mesoscopic superconducting aluminum loops near their transition temperature, in the absence of external current. Since then two mains series of experiments have been conducted. The first (Series I) [33, 32] were to verify Zhilyaev's initial results in light of new theoretical understanding [35], and the second, more detailed series (Series II) examined multi-ring systems and the effects of external ac driving [31]. We will review each.

4.4.3.1 Series I

Series I experiments were conducted on single, symmetric or asymmetric, mesoscopic, high-purity aluminum loops on silicon wafer substrates [33, 32]. Figure 4.4 is an electron micrograph of exemplary symmetric (top) and asymmetric (bottom) loops with current and voltage contacts. Structures were fashioned with electron beam lithography. Loops were 60nm thick and had diameters $2R$ =1, 2, or 4μm and linewidths $w = 0.2\mu$m and 0.4μm. The midpoint of the superconductive resistive transition was roughly $T_c \simeq 1.24$K. Measurements were carried out in a conventional helium-4 cryostat with base temperature of 1.2K. Measurements of voltage oscillations were made in the narrow temperature range

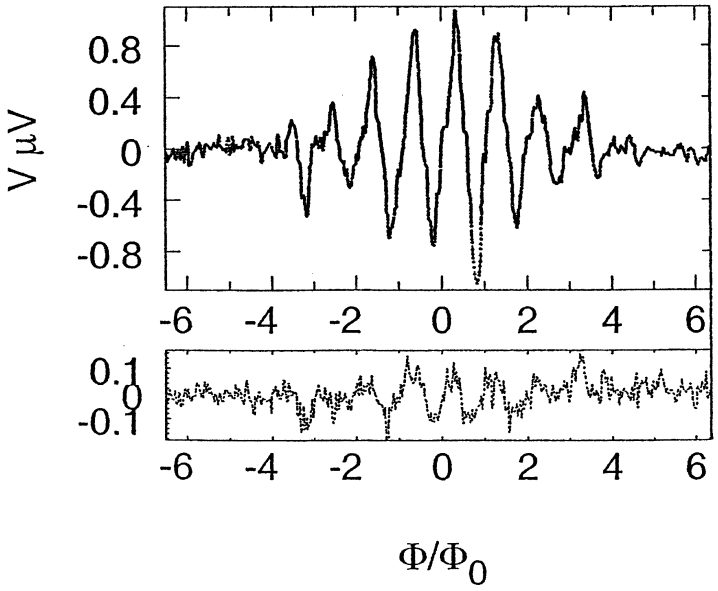

Figure 4.5: Voltage oscillation versus $\frac{\Phi}{\Phi_o}$ on single asymmetric loop measured with V_2 contacts (upper curve) and V_3 contacts (lower curve). Loop parameters: $2R = 4\mu$m, $w = 0.4\mu$m, $I_m = 0$, $T = 1.231$K at bottom of resistive transition.

$0.988T_c < T < 0.994T_c$. Loop inhomogeneity (asymmetry) was created by reducing ring linewidth.

In principle [35], the dc voltage oscillation *should not* occur in homogeneous (symmetric) loops, but *should* occur in inhomogeneous (asymmetric) loops. Experiments qualitatively confirmed this prediction.

Figure 4.5 displays the dc voltage oscillation $V(\frac{\Phi}{\Phi_o})$ versus $\frac{\Phi}{\Phi_o}$ for a single asymmetric loop ($2R = 4\mu$m, $w = 0.4\mu$m) measured at V_2 contacts (upper curve) and V_3 contacts (lower curve) at $T = 1.231$K. Voltage oscillations are observed both across the whole loop and across the segment that, because of its narrower width, was a normal conductor.

For the symmetric loop, the voltage oscillations, ($V_1 = I_1 R_1$) followed expectations of standard LP oscillations; that is, when $I_m = I_1 = 0$, the voltage oscillations disappeared ($V_1 = 0$). In contrast, the voltage oscillations on the asymmetric loop did not disappear for $I_2 = 0$. In particular, voltages of magnitude $V_3 \simeq 0.1\mu$V were observed on the asymmetric segment (Figure 4.6), when $I_2 = 0$. This was observed in the narrow temperature range at the bottom of the resistive transition $\Delta T = T - T_c \simeq 0.1$K. (Larger V_3 were observed at lower temperatures.) This stark difference in behavior between symmetric and asymmetric loops agrees with theoretical predictions [35].

The researchers raise the caution that external noise — rather than purely thermal fluctuations — cannot be ruled out as a cause for the observed dc voltages. This issue partially motivated the next series of experiments.

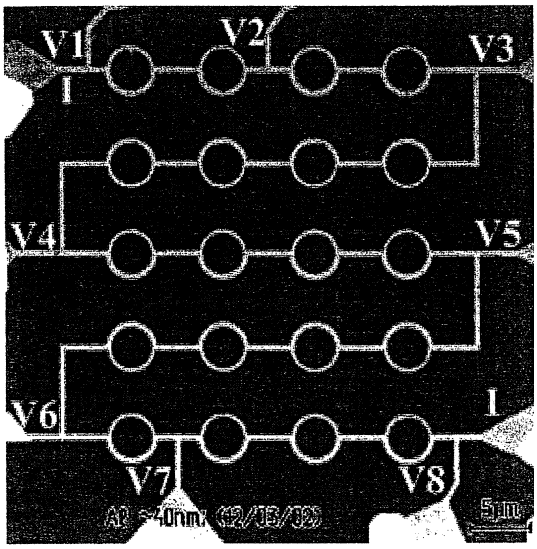

Figure 4.6: Electron micrograph of array of 20 asymmetric aluminum loops for Series II experiments. Current ΔI imposed through $I - I$ contacts. Voltage contacts $V1 - V8$.

4.4.3.2 Series II

Series II experiments were conducted on systems of either 3 or 20 asymmetric mesoscopic aluminum loops, again deposited on Si wafers and fashioned using electron beam lithography [31]. Figure 4.6 shows an array of 20 loops. All loops had diameters $2R = 4\mu$m and thicknesses 40nm. The inhomogenities (asymmetries) consisted of having one half of each loop drawn with linewidth $w = 0.2\mu$m and the other with $w = 0.4\mu$m. Resistance and current oscillations were studied in the range $0.95T_c < T < 0.98T_c$, where T_c is the midpoint of the superconducting resistive transition, $T_c \simeq 1.3$K.

As in Series I, measurements were performed in a helium-4 cryostat and a magnetic field was applied perpendicularly to the rings by a superconducting coil. Unlike Series I, the rings were driven by an external ac current, $I_{ac} = \Delta I sin(2\pi f_{ac} t)$ in the range 10^2Hz$\leq f_{ac} \leq 10^6$Hz, with amplitude 0μA$\leq \Delta I \leq 50\mu$A between contacts $I - I$ in Figure 4.6. I_{ac} was used to understand how noise (thermal or spurious background) induces voltages in the loops. Voltages were measured between contacts labeled $V1 - V8$ in Figure 4.6, thus allowing summation of voltages in series loops to be tested.

DC-voltage oscillations were measured across single and multiple loops at various magnetic field strengths ($B = \Phi/\pi R^2$) as a function of ac-current magnitude ΔI and frequency f_{ac}. The magnitude of voltage oscillations $V(\frac{\Phi}{\Phi_o})$ was found to be independent of f_{ac} over the frequency range explored ($10^2 - 10^6$Hz), but was highly dependent on ΔI. (Independence of dc voltage from f_{ac} is not sur-

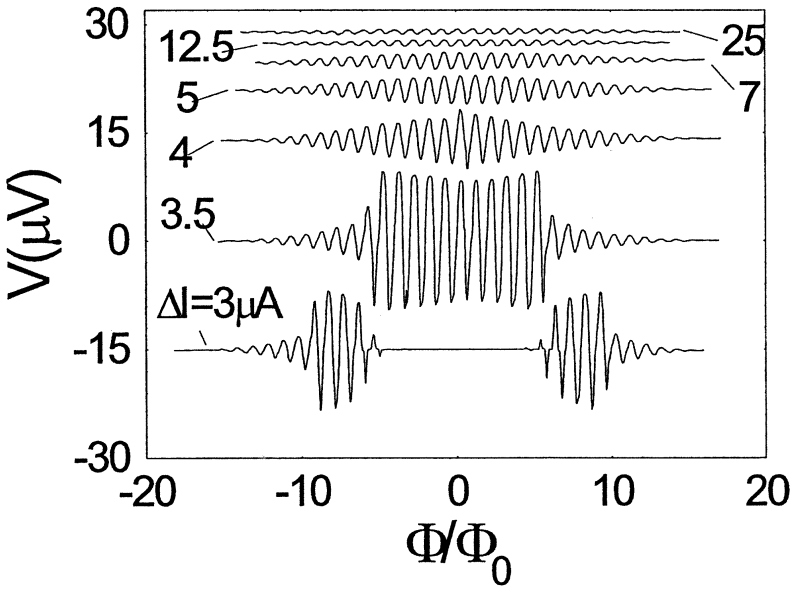

Figure 4.7: Voltage oscillation $V(\frac{\Phi}{\Phi_o})$ on a single asymmetric loop versus $\frac{\Phi}{\Phi_o}$ for different magnitudes of I_{ac} at $f_{ac} = 2.03$kHz and $T = 1.280\text{K} = 0.97T_c$. All traces except $\Delta I = 3.5\mu$A are displaced vertically.

prising since, compared with the maximum possible switching frequency ($f_{max} \sim 10^{11} - 10^{12}$Hz), the ratio $f_{ac}/f_{max} \sim 0$, such that the driving field is effectively static.)

Figure 4.7 displays plots of $V(\frac{\Phi}{\Phi_o})$ versus $\frac{\Phi}{\Phi_o}$ across a single loop for seven values of ΔI at temperature $T = 1.280$K and frequency $f = 2.03$kHz. For all traces, at large values of Φ/Φ_o (*i.e.*, $\mid \Phi/\Phi_o \mid \geq 10$), one has $V \sim 0$ because of the supression of superconductivity at high imposed field values. The lowest trace ($\Delta I = 3\mu$A) displays no $V(\frac{\Phi}{\Phi_o})$ voltage oscillations below a critical threshold current, ΔI_{cr} for $\mid \Phi/\Phi_o \mid \leq 5$. As the imposed field is increased, the critical current ΔI_{cr} is reduced so that voltage oscillation appear. As noted earlier, however, they disappear again at $\mid \Phi/\Phi_o \mid \geq 10$ as the aluminum superconductivity is supressed by the imposed field.

On the next trace up ($\Delta I = 3.5\mu$A), the voltage oscillations are most robust, just beyond the critical threshold current. For large values of ΔI beyond ΔI_{cr}, the voltage oscillations (higher vertical traces in Figure 4.7) again decrease proportionately because of suppression by ΔI-induced magnetic fields.

Loop oscillation voltages can be summed in series. In Figure 4.8, voltage oscillations $V(\frac{\Phi}{\Phi_0})$ are plotted versus Φ/Φ_0 for two series cases: 3 loops and 20 loops. A comparison is less quantitative than desired since the experimental parameters are distinct for each case (See Figure 4.8 caption for details.), but a trend is evident: The ΔV magnitudes for 20 loops is on the order of 7 times greater than for 3 loops, which in turn is roughly 3 times greater than for 1 loop (Figure 4.4).

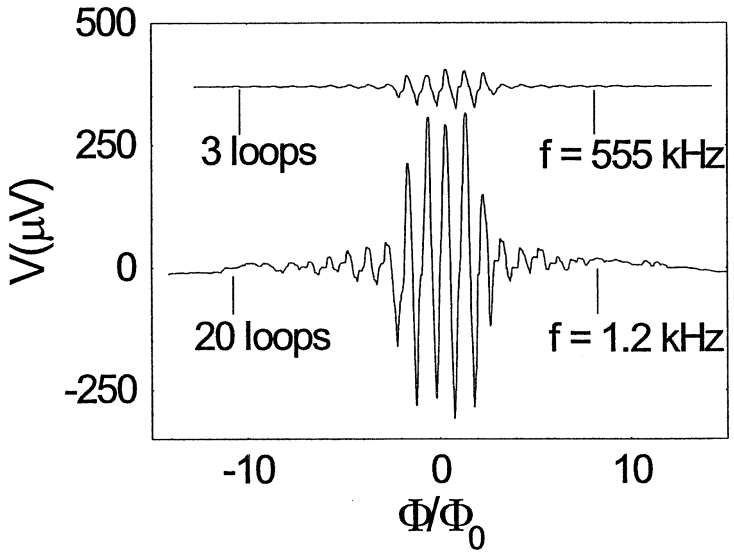

Figure 4.8: Series summation of loop voltage oscillations for 2 loop arrays. 20-loop array [f_{ac} = 1.2kHz, $\Delta I = 3.2\mu$A, $T = 1.245\text{K}=0.97T_c$]; 3-loop array [$f_{ac}$ = 555kHz, $\Delta I = 4.5\mu$A, $T = 1.264\text{K}=0.96T_c$].

Specifically, voltage oscillations were observed up to 10μV for a single loop, up to 40μV for 3 loops in series and up to 300μV for 20 loops in series.

The quantum oscillations in Figures 4.7 and 4.8 can be attributed to loop switchings between superconducting states with different connectivity, as induced by the external current [31], whereas those in Figure 4.5 possibly could be induced by external electrical noise. Neither result directly contradicts the second law because the source of the observed dc power is not equilibrium thermal fluctuations. However, it is significant that the dc voltages observed on Figures 5,7,8 are induced by loop switchings near the critical temperature $T \approx T_c$, thereby corroborating a key aspect of the theory.

Recent theoretical and numerical work by Berger [30] lends strong qualitative support to the experimental work of Dubonos, Nikulov, et al. [31-37]. Berger studied a superconducting loop with two, unequal weak links. The loop was held near T_c and was threaded with magnetic flux. Although it does not match Nikulov's system exactly, it does bear strong physical similarities. Furthermore, it can be modeled by textbook procedures for Josephson junctions and can be compared directly to related work on Josephson rectifying ratchets [38, 39, 40].

Berger found that when loop superconductivity was broken by thermal fluctuations and resistive noise (in the vicinity of T_c), the average dc loop voltage *did not* vanish and showed qualitatively the same $V(\frac{\Phi}{\Phi_0})$ versus Φ/Φ_0 flux dependence and the same frequency independence as was predicted and observed by Nikulov, et al. He also reported the same $V(\frac{\Phi}{\Phi_o})$ dependence in the presence of ac current ΔI. (Compare, for example, Figure 4.5 in [30] with Figure 4.6 [31].)

It is stressed that, while Berger's study shows strong qualitative agreement with the fundamental processes predicted and observed by Dubonos, Nikulov, et al., the quantitative agreement is poor. Some of these differences might be attributable to the differences in the models.

4.4.4 Discussion

The theory and experiments by Nikulov, Dubonos, et al. — and their further independent theoretical corroboration by Berger [30] — represent a cogent challenge to the second law. Conclusive violation, however, cannot be claimed for several reasons. First, only one of the physical variables necessary to establish dissipation was measured experimentally; the other was inferred from theory. Ideally, both should be measured simultaneously by independent means. Second, an unambiguous experimental measurement of dissipation (local heating or radiation emission) should be made and, ideally, some global accounting of energy (work plus heat) should be carried out. Third, in no experiment has it been clearly established that thermal fluctuations were the source of the experimentally measured voltage oscillations and inferred persistent currents. Fourth, the experimental apparatus and experimenter surely generated far more entropy than could be negated by the loops.

The extreme experimental and physical requirements of this system (helium-4 cryostats, vacuum systems, microscale fabrication) probably make it commercially impractical unless perhaps high-temperature superconductors can be employed. On the other hand, as an experimentally-based challenge, it holds much promise.

4.5 Bose-Einstein Condensation and the Second Law

Keefe's and Nikulov's paradoxes share deep similarities. Both capitalize on the normal-to-superconducting transition — the transition from classical mechanical to quantum mechanical behavior — and both operate at the borderline between the two. In many respects, they can be considered quantum thermal ratchets. Keefe's CMCE engine exploits the transition induced by magnetic field strength near the critical field (H_c) and, in its primary incarnation, delivers mechanical work. Nikulov's inhomogeneous mesoscopic loop exploits the transition induced by thermal fluctuations near the critical temperature (T_c) and delivers electrical work. Both exploit the exigency of Bose-Einstein condensation and the persistent current[3]: the spontaneous drive to order as the system falls into a single, macroscopic quantum state. In Keefe's case, this order is found in the diamagnetic persistent current of the Meisner-Oschenfeld effect whereby mechanical work is extracted as the armature is expelled from the high field region. In Nikulov's case,

[3] Persistent currents have been claimed in normal metal [41] and semiconductor [42] mesoscopic loops.

again the order is in the form of a supercurrent, this time summoned by thermal fluctuations via the Little-Parks effect.

In light of their simularities, these two challenges suggest a deeper, unifying principle may be connecting them. They also suggest a fundamental limitation to the second law in processes involving the transition from classical mechanical to quantum behavior. Nikulov's *quantum force* may hint at this deeper principle, but it possibly does not go deep enough [22]. At a more fundamental level, the behavior of bosons in Bose-Einstein condensation is antipodal to the behavior of fermions subject to Pauli exclusion. The former intrinsically moves a multiparticle system toward a state of low entropy (single wavefunction), while the latter guarantees a state of relatively high entropy (no two particles in the same state). Neither quantum tendency arises from thermodynamic action; rather, both emerge from the purely quantum mechanical consideration of wavefunction parity.

Most classical systems are dominated by Fermi statistics and Pauli exclusion, rather than by Bose-Einstein statistics or condensation. Given their antipodal thermodynamic tendencies, perhaps it is not surprising that these two second law challenges arise only in systems involving transitions between classical and quantum statistics.

4.6 Quantum Coherence and Entanglement

4.6.1 Introduction

Allahverdyan, Nieuwenhuizen, et al. have written extensively on the limits to various formulations of the second law in the quantum regime, particularly quantum coherence and entanglement. They have been among the most fastidious in recognizing that different formulations can mean different things and that one must be cognizant of the caveats and limitations of each. They have championed the Thomson formulation — *No work can be extracted from a closed equilibrium system during a cyclic variation of a parameter by an external source* — because its basic currency (work) is a well-defined physical quantity, whereas heat and entropy (the more common currencies) are less well-defined and can be context dependent[4]. (These researchers have also shown recently that the quantum mechanical effect of level crossing limits the minimum work principle and that adiabatic procesess do not correspond to optimal work if level crossing occurs [43].)

At this time, the hypotheses that quantum coherence or quantum entanglement can lead to violations of various formulations of the second law remain experimentally untested and largely uncorroborated; however, several concepts for experiments have been advanced. We will summarize the two most detailed of these by Pombo, et al. [44] and Allahverdyan and Nieuwenhuizen [45].

[4]It is stressed that Allahverdyan, et al. have never claimed violation of the Thomson formulation, but rather, have proved its inviolability for systems starting in equilibrium (§3.4).

4.6.2 Spin-Boson Model

Pombo, et al. [44] propose several general schemes by which two-level systems (modeled as spins) that are quantum mechanically entangled with a bath of harmonic oscillators can extract work from a heat bath. Two-level systems are ubiquitous in nature and technology and are among the most studied quantum systems known. These include nuclear magnetic resonance (NMR), electron spin resonance (ESR) and spintronic systems, two-level Josephson junctions, electrons in quantum dots, and two-level atoms [46, 47].

Pombo, et al. analyse a spin-boson model, which approximates the behavior of several systems listed above, and which also is exactly solvable analytically [46, 47]. The Hamiltonian for a system consisting of a spin 1/2 particle interacting with a bath of harmonic oscillators can be written

$$\mathcal{H} = \mathcal{H}_S + \mathcal{H}_B + \mathcal{H}_I, \tag{4.19}$$

where

$$\mathcal{H}_S = \frac{\epsilon}{2}\hat{\sigma}_z + \frac{\Delta(t)}{2}\hat{\sigma}_x; \quad \mathcal{H}_B = \sum_k \hbar\omega_k \hat{a}_k^\dagger \hat{a}_k; \quad \mathcal{H}_I = \frac{1}{2}\sum_k g_k(\hat{a}_k^\dagger + \hat{a}_k)\hat{\sigma}_z. \tag{4.20}$$

Here $\mathcal{H}_{B,S,I}$ are the Hamiltonians for the bath, the spin-1/2 particle, and their interaction. $\hat{\sigma}$ are the Pauli spin matrices; $\hat{a}_k^\dagger$ and $\hat{a}_k$ are creation and annihilation operators; g_k are the coupling constants between the bath modes and the spin; and $\epsilon = \bar{g}\mu_B B$ is the standard energy of a spin in a magnetic field, where μ_B is the Bohr magneton, $\bar{g}$ is the gyromagnetic constant and B is the magnetic field. $\Delta(t)$ is an interaction potential that is switched on and off quickly from an external source and affects the x-component of spin.

Various modes and protocols of interaction between spin and bath are discussed [44]. We consider an archetypical one in which the spin is subjected to a sudden, brief external pulse, by which the spin is quickly driven about the x-axis. (Here $\Delta \neq 0$ lasts for duration δ_1 and has large magnitude; *i.e.*, $\Delta \sim \frac{1}{\delta_1}$.) In principle, this can be accomplished without changing the energy of the spin ϵ since energy depends on $\hat{\sigma}_z$ and not $\hat{\sigma}_x$. The time-evolution operator associated with the pulse is: $\hat{U}_1 \equiv exp\left[-i\frac{\mathcal{H}t}{\hbar}\right] = exp\left[-i\frac{\mathcal{H}\delta_1}{\hbar}\right]$, which, in this approximation ($\Delta \sim \frac{1}{\delta_1}$), can be written $\hat{U}_1 \simeq exp\left[\frac{i}{2}\Theta\hat{\sigma}_x\right] + \mathcal{O}(\delta_1)$, where $\Theta = -\frac{\delta_1\Delta}{\hbar}$, the x-rotation angle. Note, pulses correspond to a cyclic process of an external work source and they change neither the energy of the spin, nor its statistical (von Neumann) entropy.

Although the energy of the spin need not change during on-off switching of $\Delta(t)$, the total system work involves both the spin *and* bath and it is found that work can be extracted from the heat bath with proper pulsing of $\Delta(t)$. Under the conditions that g is small, $\Theta \equiv -\frac{\delta_1\Delta}{\hbar} = -\frac{\pi}{2}$; and $t \gg \frac{1}{\Gamma}$ = the relaxation time of the bath; and $\epsilon = 0$ (to insure the spin energy does not change), the added work is given by

$$W_1 = \frac{g\hbar\Gamma}{2\pi} + \frac{gkT}{2}\langle\hat{\sigma}_x(0)\rangle exp\left[-\frac{t}{\tau_2}\right], \tag{4.21}$$

where kT is bath thermal energy and τ_2 is the transversal ($\hat{\sigma}_x$) spin decay time. If the spin starts in a coherent state ($\langle\hat{\sigma}_x\rangle = -1$) and if the time is adjusted such that $\frac{kT}{2}exp[-\frac{t}{\tau_2}] > \frac{\hbar\Gamma}{2\pi}$, then (4.21) indicates work can be extracted from the bath ($W_1 < 0$). This demonstrates that the Thomson formulation cannot be applied to the locally equilibrium heat bath. However, it is applicable if the whole system — *i.e.* the spin and bath together — starts in equilibrium before applying the first pulse. (Other schemes challenge the Clausius inequality, whereby work can be extracted from the bath without changing the entropy of the spin [44].)

Pombo, et al. offer several incentives for pursuing laboratory experiments:
1) Two-level quantum systems and harmonic oscillator heat baths are ubiquitous, within appropriate physical limits [46, 47], *e.g.*, atoms in optical traps, electron spins in semiconductors (injected or photonically excited), excitons in quantum dots, nuclear spins (NMR), or electron spins (ESR) in condensed matter.
2) Experimental detection methods are, in principle, sufficiently well-developed (*e.g.*, ESR, NMR) to make the salient measurements.
3) The main quantum effects survive for completely disordered ensembles of spins.

4.6.3 Mesoscopic LC Circuit Model

Electrical circuits have long been fertile testbeds for thermodynamics and statistical mechanics [48, 49]. Recently, Allahverdyan and Nieuwenhuizen have suggested experiments on mesoscopic or nanoscopic, linear LRC circuits interacting with a low-temperature heat bath, which in principle could test for predicted violations of the Clausius form of the second law in the quantum regime [45].

A classical series LRC circuit can be described in terms of conjugate variables (charge (Q) and magnetic flux (Φ)). These play roles analogous to canonical coordinate and momentum in a mass-spring system. Written side by side the LRC circuit and mass-spring Hamiltonians are written (for zero-damping):

$$H_s = \frac{\Phi^2}{2L} + \frac{Q^2}{2C}; \quad H = \frac{p^2}{2m} + \frac{kx^2}{2} \tag{4.22}$$

From inspection, $p \equiv \Phi$, $m \equiv L$, $k \equiv \frac{1}{C}$; and $x \equiv Q$. Note that the conjugate variables are also related analogously: $\dot{Q} = \frac{\Phi}{L}$ and $\dot{x} = \frac{p}{m}$. For the $R = 0$ case, this classical system can be treated quantum mechanically by allowing Q and Φ to act as operators satisfying the commutation relation: $[Q, \Phi] = i\hbar$.

In either the classical or quantum regimes, a measure of a circuit's disorder (entropy) can be taken to be the volume of phase space (Σ) that it explores. In terms of the LRC circuit variables, this can be written

$$\Sigma = \frac{\Delta\Phi\Delta Q}{\hbar} \equiv \sqrt{\frac{\langle\Phi^2\rangle\langle Q^2\rangle}{\hbar^2}} \tag{4.23}$$

where $\langle\Phi^2\rangle$ and $\langle Q^2\rangle$ are the dispersions (variances) in Φ and Q. In the classical thermodynamic limit, the dispersions take the Gibbsian forms:

$$\langle \Phi^2 \rangle_G = \frac{1}{2} L\hbar\omega_o \tanh(\frac{1}{2}\beta\hbar\omega_o) \tag{4.24}$$
$$\langle Q^2 \rangle_G = \frac{1}{2} C\hbar\omega_o \tanh(\frac{1}{2}\beta\hbar\omega_o)$$

where $\omega_o = \frac{1}{\sqrt{LC}}$ is the undamped LC resonance frequency, and $\beta = \frac{1}{kT}$ is the inverse thermal energy.

Starting from the quantum Langevin equations and assuming quantum Gaussian noise with the Nyquist spectrum having a large cut-off frequency ($\omega_{max} \equiv \Gamma$) [50], the quantum dispersions in Φ and Q can be written

$$\langle \Phi^2 \rangle = \int \frac{d\omega}{2\pi} \frac{\omega^2 k(\omega)}{(1+\frac{\omega^2}{\Gamma^2})\left[(\omega^2-\omega_o^2)^2 + (\frac{\omega R}{L})^2\right]} \tag{4.25}$$
$$\langle Q^2 \rangle = \int \frac{d\omega}{2\pi} \frac{k(\omega)}{[(\omega^2-\omega_o^2)^2 L^2 + (\omega R)^2]}$$

with $k(\omega) = \hbar R\omega \; coth(\frac{\hbar\omega}{2kT})$.

Comparing (4.24) with (4.25), it is clear that the quantum and classical dispersions are distinct. Notably, the quantum dispersions include damping (R), whereas the classical dispersions do not. In the limit of weak coupling with the heat bath ($R \to 0$) or at high temperatures ($\frac{\hbar\omega}{kT} \to 0$), the quantum cases revert to the classical Gibbsian cases.

The Clausius formulation of the second law can be phrased in the form of the Clausius inequality: $dQ \leq TdS$. The heat and entropy changes can also be expressed in terms of changes in phase space volume $d\Sigma$, which in turn can be written in terms of physically measurable variances Q and Φ through (4.23-25). Classically, if the LRC circuit absorbs heat from the heat bath, then its phase space volume will expand; conversely, if heat is lost to the heat bath, its phase space volume will contract. If the dispersions $\langle Q^2 \rangle$ and $\langle \Phi^2 \rangle$ are Gibbsian, then classical thermodynamics applies and the Clausius criterion $dS \geq \frac{dQ}{T}$ is satisfied. However, if the temperature is sufficiently low, then the dispersions follow the quantum prescriptions, (4.25), and as Allahverdyan and Nieuwenhuizen have shown, in this regime the Clausius form of the second law can be violated [51, 52]. In this case, the circuit can absorb heat from the bath while simultaneously contracting in phase space. More precisely, at finite temperatures a cloud of electromagnetic modes forms around the LRC circuit. Its energy should be counted to the bath and may be partly harvested since changing a parameter of the LRC circuit can induce a change in this cloud.

For the LRC circuit, in principle, this second law violation would be realized by varying a system parameter (say, inductance L) via an external agent and, thereby, affecting the heat transferred from the heat bath to the circuit. In the quantum regime, they find that for low quality factor circuits,

$$dQ = \frac{\hbar R}{2\pi L^2} dL > 0 \tag{4.26}$$

and that $\frac{d\Sigma}{dL} < 0$; that is, there is positive heat transfer to the circuit and phase space contraction. These constitute violations of the Clausius form of the second law.

Unlike the classical Clausius constraint ($dQ \leq TdS$), which requires non-zero temperature for heat transfer, this quantum constraint for heat transfer from bath to system is temperature independent; therefore, in principle, it can occur at zero temperature. This observation spotlights the defining characteristic of this quantum thermodynamic system: the role of entanglement. At first consideration, a heat bath at $T = 0$ should not be able to render up heat since presumably it is in its ground state, possessing only zero-point energy. Equation (4.26) indicates, however, that heat can in fact be rendered from the bath at zero temperature. Appealing to the first law, one concludes that the bath is *not* in its ground state. In fact, because it is always entangled with the circuit — and, therefore, in a mixed state — it is never in its true ground state. This extra *entanglement energy* has no classical analog and lies at the heart of this quantum second law challenge. This entanglement leads to a screening cloud, known elsewhere as a Kondo cloud or polaronic cloud. Not surprisingly, these also arise in some of Čápek's systems (§3.6). Nieuwenhuizen and Allahverdyan speculate that such clouds may well be the sole cause underlying the differences between classical and quantum thermodynamics.

Experimental support for this challenge would consist in measuring heat flow from the heat bath into the LRC circuit while simultaneously measuring decreases in the dispersions $\langle \Phi^2 \rangle$ and $\langle Q^2 \rangle$. Experiments on low-temperature mesoscopic tunnel junctions have reported inferred values of $\langle Q^2 \rangle$ in related sub-Kelvin temperature regimes [53, 54], thus offering hope that full-fledge tests of the Clausius inequality might be possible. Such experiments would be difficult to design, conduct, and interpret, but they appear within the current experimental art.

4.6.4 Experimental Outlook

The above-mentioned experimental concepts and incentives are compelling and should be pursued more fully since they offer the hope of sensitive tests of at least two formulations of the second law (Thomson and Clausius) on many systems for which there is already deep understanding. On the other hand, the level of theoretical analysis and experimental details presented for the experiments thus far [44, 45] are insufficient to determine whether such experiments are truly feasible or even whether their proposed thermodynamic cycles can achieve breakeven in entropy reduction. Let us consider theory first.

The analysis of Pombo's thermodynamic cycle appears incomplete, leaving out key thermodynamic steps. For instance, the work and entropy generation required to prepare the $\langle \hat{\sigma}_x(0) \rangle = -1$ state has not been assessed, although τ_2 is admittedly finite, such that spins must be restored on a regular basis for the cycle to repeat. (If, on the other hand, random spins are used, then the conditions for (4.21) to return strictly negative work ($W_1 < 0$) appear compromised since $W_1 < 0$ requires the simultaneous tuning of phase-dependent parameters. Or, if random spins are used judiciously, these spin states must be measured, presumably by an energy-consuming, entropy-generating agent.) Additionally, no assessment has

been made of the work or entropy generation associated with the nonequilibrium Δ pulse that couples the spin and bath. Similarly, for the quantum LRC circuit no thermodynamic assessment has been made of the dL-varying agent[5]. In short, several key elements of this cycle have not been assessed thermodynamically. On the other hand, if the experiments aim merely to test for the fundamental effects — full second law challenges aside — then these objections may be moot.

There are also many experimental issues that have not been addressed — too many to list here — so let this summarize: No realistic experimental system for either proposal (spin-boson or LRC) has explicitly been shown to meet the criteria for work extraction from a heat bath, nor have explicit experimental designs with realistic experimental parameters been vetted adequately. For neither model has it been well-established that experimental techniques are adequate to make the necessary measurements, nor that the negentropy of the cycle can outweigh the the entropy production of the apparatus, even in principle. In contrast, Nikulov, et al. (§4.4), Keefe (§4.3), and Sheehan (Chapters 7-9) have treated well-defined experimental circumstances, realizing that with experiments, *the devil is in the details*. In summary, within the idealizations of their theoretical development, compelling cases have been made for second law challenges in the quantum regime; however, these experiments are still in the conceptual stage.

The thermodynamic requirements for these and the previous challenges (§4.3, §4.4) are extreme. The superconducting ones require both low-temperatures and micro- or mesoscopic structures, which burden experimental techniques and hamper direct, unambiguous measurements of predicted entropy reductions or heat fluxes — whichever is necessary. It is not enough for the CMCE engine to simply run, or for voltage oscillations to be measured in an inhomogeneous superconducting loop near its transition temperature. To challenge the second law successfully, the involvement of *all* other possible free energy sources must be ruled out and, ideally, direct measurements must be made of sustained heat fluxes or entropy reductions that are causally connected to the forbidden work. These types of energy and entropy determinations are not trivial even for room-temperature, everyday macroscopic devices like flashlights; thus, for a vacuum-packed, microscopic superconductor near absolute zero, it is likely to be more difficult. With regard to the entanglement proposals, here the difficulties associated with microscopic devices are traded for the intricacies and uncertainties associated with entanglement. As a simple example, how does one quantitatively measure system-bath entanglement and demonstrate unambiguously that it has been transformed into work?

Despite these hurdles, these low-temperature challenges are among the most compelling of the modern era. At a deep level they underscore the fundamental differences between classical and quantum thermostatistical behaviors. Of course, quantum statistics were unknown at the time thermodynamics and statistical mechanics were being forged, and since then quantum systems have grown up to be disrespectful of the zeroth and third laws. Perhaps it should not be too surprising that they now show occasional disrespect for the second.

[5] In principle, a work source generates negligible entropy, but for real experimental systems this is rarely the case.

References

[1] Meissner, W. and Ochsenfeld, R., Naturwiss. **21** 787 (1933).

[2] Tinkham, M., *Introduction to Superconductivity* (McGraw-Hill, New York, 1975).

[3] Langenberg, D.N. and R.J. Soulen, Jr. in *McGraw-Hill Encyclopedia of Science and Technology*, 7^{th} ed., Vol. 17, (McGraw-Hill, New York, 1992) pg. 641.

[4] Kittel, C., *Introduction to Solid State Physics*, 7^{th} Ed., Ch. 12, (Wiley, New York, 1996).

[5] Bardeen J., Cooper L.N., Schrieffer J.R., Phys. Rev. **108** 1175 (1957).

[6] Ginzburg, V.L. and Landau, L.D., Zh. Eksp. Teor. Fiz. **20** 1064 (1950)

[7] Hauser, J.J., Phys. Rev. B **10** 2792 (1974).

[8] Salamon, M.B., in *Physical Properties of High Temperature Superconductors I*, Ginsberg, D.M., Editor, (World Scientific, Singapore, 1989).

[9] Huebener, R.P., *Magnetic Flux Structures in Superconductors* (Springer-Verlag, Berlin, 1979).

[10] Abrikosov, A.A., Zh. Eksp. Teor. Fiz. **32** 1442 (1957); (*Sov. Phys.-JETP* **5** 1174 (1957)).

[11] Marchenko, V.A. and Nikulov, A.V., Pisma Zh. Eksp. Teor. Fiz. **34** 19 (1981); (JETP Lett. **34** 17 (1981)).

[12] Nikulov, A.V., Supercond. Sci. Technol. **3** 377 (1990).

[13] Safar, H., Gammel, P.L., Huse, D.A., Bishop, D.J., Rice, J.P. and Ginzberg, D.M., Phys. Rev. Lett. **69** 824 (1992).

[14] Trupp, A., in *Quantum Limits to the Second Law*, AIP Conf. Proceed. Vol. 643, Sheehan, D.P., Editor, (AIP Press, Melville, NY, 2002) pg. 201.

[15] Pippard, A.B., Phil. Mag. **43** 273 (1952).

[16] Lutes, O. and Maxwell, E., Phys. Rev. **97** 1718 (1955).

[17] Geim, A.K., Dubonos, S.V., Lok, J.G.S., Grigorieva, I.V., Maan, J.C., Hansen, L.T., and Lindelof, P. E., Appl. Phys. Lett. **71** 2379 (1997).

[18] Geim, A.K., Dubonos, S.V., Palacios, J.J., Grigorieva, I.V., Henini, M., and Schermer J.J., Phys. Rev. Lett. **85** 1528 (2000); Geim, A.K., Dubonos, S.V., Grigorieva, I.V., Novoselov, K.S., Peeters, F.M., and Schweigert V.A., Nature **407** 55 (2000).

[19] Little, W.A. and Parks, R.D., Phys. Rev. Lett. **9** 9 (1962).

[20] Vloeberghs, H., Moshchalkov, V.V., Van Haesendonck, C., Jonckheere, R. and Bruynseraede, Y., Phys. Rev. Lett. **69**, 1268 (1992).

[21] Tinkham, M., Phys. Rev. **129** 2413 (1963).

[22] Nikulov, A.V., Phys. Rev. B **64** 012505 (2001).

[23] Keefe, P., in *Quantum Limits to the Second Law*, AIP Conf. Proceed. Vol. 643, (AIP Press, Melville, NY, 2002) pg. 213.

[24] Keefe, P., J. Appl. Optics **50** 2443 (2003); Entropy **6** 116 (2004).

[25] Chester, M., J. Appl. Phys. **33** 643 (1962).

[26] Keefe, P., Masters Thesis, University of Detroit, MI (1974).

[27] Bryant, C. and Keesom, P., Phys. Rev **123** 491 (1961).

[28] Roukes, M.L., *Tech. Dig. of the 2000 Solid-State Sensor and Actuator Workshop*, Hilton Head Isl. SC, June (2000).

[29] Caswell, H.,J., Appl. Phys. **36** 80 (1965).

[30] Berger, J., http://xxx.lanl.gov/abs/cond-mat/0305130; in press Phys. Rev. B **70** (2004).

[31] Dubonos, S.V., Kuznetsov, V.I., Zhilyaev, I.N., Nikulov, A.V., and Firsov, A.A., JETP Lett. **77** 371 (2003).

[32] Dubonos, S.V., Kuznetsov, V.I., and Nikulov, A.V., in *Proceedings of 10th International Symposium "Nanostructures: Physics and Technology,"* St. Petersburg Ioffe Institute, (2002) pg 350.

[33] Nikulov, A.V., in *Quantum Limits to the Second Law*, AIP Conference Vol. 643, (AIP Press, Melville, NY, 2002) pg. 207.

[34] Aristov, V.V. and Nikulov A.V., in *Quantum Informatics*, Proceedings of SPIE Vol. **148** 5128 (2003);
http://xxx.lanl.gov/abs/cond-mat/0310073

[35] Nikulov, A.V. and Zhilyaev, I.N., J. Low Temp. Phys. **112** 227 (1998).

[36] Barone, A. and Paterno, G., *Physics and Applications of the Josephson Effect* (Wiley-Interscience, New York, 1982).

[37] Nikulov, A.V., in *Supermaterials*, Cloots, R., et al., Editors, Proceedings of the NATO ARW, (Kluwer Academic, 2000) pg. 183.

[38] Zapata, I., Bartussek, R., Sols, F., and Hänggi, P., Phys. Rev. Lett **77** 2292 (1996).

[39] Falo, F, Martinez, P.J., Mazo, J.J., and Cilla, S., Europhys. Lett. **45** 700 (1999).

[40] Weiss, S., Koelle, D., Müller, J., Gross, R., and Barthel, K., Europhys. Lett **51** 499 (2000).

[41] Levy, L.P. et al., Phys. Rev. Lett. **64** 2074 (1990); Chandrasekhar, V. et al., Phys. Rev. Lett. **67** 3578 (1991); Jariwala, E.M.Q. et al., Phys. Rev. Lett. **86** 1594 (2001).

[42] Mailly, D., Chapelier, C. and Benoit, A., Phys. Rev. Lett. **70** 2020 (1993); Reulet, B. et al, Phys. Rev. Lett. **75** 124 (1995); Rabaud, W. et al., Phys. Rev. Lett. **86** 3124 (2001).

[43] Allahverdyan, A.E. and Nieuwenhuizen, Th.M, cond-mat/0401548.

[44] Pombo, C., Allahverdyan, A.E., and Nieuwenhuizen, Th.M. in proceedings of *Quantum Limits to the Second Law*, AIP Conference Proceedings, Vol. 643 (AIP Press, Melville, NY, 2002) pg. 254; Allahverdyan, A.E. and Nieuwenhuizen, Th.M., J. Phys. A: Math. Gen. **36** 875 (2004).

[45] Allahverdyan, A.E. and Nieuwenhuizen, Th.M., Phys. Rev. B **66** 115309 (2003).

[46] Leggett, A.J., et al., Rev. Mod. Phys. **59** 1 (1987).

[47] Luczka, J., Physica A **167** 919 (1990).

[48] Nyquist, H., Phys. Rev. **32** 110 (1928).

[49] Brillouin, L., Phys. Rev. **78** 627 (1950).

[50] Weiss, U., *Quantum Dissipative Systems* (World Scientific, Singapore, 1999).

[51] Allahverdyan, A.E. and Nieuwenhuizen, Th.M., Phys. Rev. Lett. **85** (2000); Nieuwenhuizen, Th.M. and Allahverdyan, A.E., Phys. Rev. E **66** 036102 (2002).

[52] Allahverdyan, A.E. and Nieuwenhuizen, Th.M., Phys. Rev. E **64** 056117 (2001).

[53] Cleland, A.N., Schmidt, J.M., and Clarke, J., Phys. Rev. B **45** 2950 (1992).

[54] Hu, G.Y. and O'Connell, R.F., Phys. Rev. B **46** 14219 (1992).